Droop Method for High-Capacity Parallel Inverters using Virtual Impedance

Kyosun Jung, Kyungbae Lim, Donghwan Kim, and Jaeho Choi
Chungbuk National University, Republic of Korea

***Abstract*--In this paper, the droop controlled parallel inverter systems with virtual inductor is considered under the unequal resistive-inductive combined line impedance condition which causes the reactive power sharing error. Here, the reactive power sharing error can be reduced by considering each line impedance voltage drop. But if the parallel inverter system is in high power level with large output current, the magnitude of reference output voltage becomes extremely lower than the rated voltage magnitude value because of the virtual inductance high voltage drop due to the multiplication with large output current. Hence, not only the line impedance voltage drop but also the virtual inductance voltage drop has been added to the conventional droop equation so that parallel inverters operate within the range of rated output voltage. Finally, the proposed droop method has been verified by comparing with conventional method through the PSIM simulation.**

***Index Terms*—Parallel inverter, droop control method, virtual inductor, islanded mode, power sharing, distributed generation (DG)**

I. INTRODUCTION

DG (Distributed generation) is connected to the main grid by the multiple small-scale generations located near the local loads. The flexible operation of full system is possible because DG improves the accessibility of local load and realizes the local control of DG [1]. Here, Microgrid is the integration of these DGs such as photovoltaic, wind power, fuel cell, etc. So Microgrid is in contrast with the concept of centralized generation which is mainly composed of large-scale generation such as thermal power generation and nuclear power generation [1].

DG based on Microgrid operates in either grid-connected mode or islanded mode [2]. In grid-connected mode, Microgrid can be defined as a current source because it supplies to main grid with synchronizing the phase of PCC (Point of Common Coupling) voltage. But when the grid fault occurs or a strategic islanding is needed, it has to be transferred to the islanded mode by opening the static switch which connects DG to PCC. Then, Microgrid operates as a voltage source because it has to supply the full load demand only with the local DG units instead of the main grid. In this islanded, the load sharing control for parallel inverters is very important to continue not only supplying the load demand but also keeping the high power quality [1]. One method for load sharing of parallel inverters is 'Master-Slave' control [3,4]. In master-slave control, one voltage controlled PWM inverter is used as a master module and the other current controlled PWM inverters are used as a slave module. It is simple to design and implement regardless of line impedances through the communication among inverters. But this control method has a critical drawback. When a control failure occurs in the master module, the control of slave modules also fails due to the failure of control intercommunication among inverters [3]. So the control technique of parallel inverters is necessary to operate independently without any intercommunication. The frequency and voltage droop control is one of the counter methods to control the power and share the loads without communications among parallel inverters [5,6]. And it also guarantees the reliable operation of parallel inverters even under the DG unit's sudden hot swap connection. However, there are several consideration as followings [7].

1) When the line resistance cannot neglect in the distribution system, the inductive line based conventional P-ω and Q-E droop relation becomes ineffective which causes the droop control failure.

2) In parallel operation, different line voltage drops due to the different line impedances cause the reactive power sharing error.

To avoid the mutual interference between P-Q and ω-E mentioned in the above, the virtual impedance has been used to decouple the P-Q coupling by making system overall impedance dominant [7,8]. To compensate the aforementioned reactive power sharing error due to the unequal line voltage drop, the feedforward term of line voltage drop has been considered [1,7]. In these works, the calculations of line voltage drop are based on power flow analysis according to R/X value and output power. Hence, the reactive power sharing error due to the unequal line voltage drops can significantly be reduced without using the high voltage droop coefficient (Note that higher voltage droop coefficient realizes the faster dynamic and more accurate power sharing, but it can cause the system instability as increasing).

But if the system is high-capacity system of which the output current is very large, then the voltage drop of virtual impedance becomes also high [9]. Hence, the output real power will be decreased as the decrease of output voltage because of high virtual impedance voltage drop due to the large output current (Note that the virtual impedance voltage drop is obtained through the multiplication of both virtual impedance value and output current [10]). Hence, adding a feedforward term of the virtual impedance voltage drop as well as that of the line voltage drop has been considered in this paper to realize the correct sharing of rated real power.

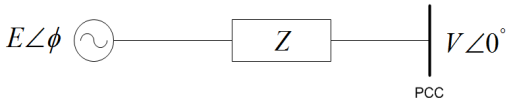

Fig. 1.Equivalent circuit of distributed generation system.

And this paper shows that it can adopt the selection method of virtual impedance for the analysis of the transient state. In [11], the complex small signal modeling has been realized with transient droop gains. But this droop coefficient has not been considered here for simple small signal modeling. Finally, the proposed droop method and the small signal modeling have been verified and analyzed through the PSIM and MATLAB simulation.

II. Droop Control and System Modeling

A. Conventional Droop Control

Figure 1 shows the equivalent circuit of distributed generation system. Here, $E\angle\phi$ isthe output voltage of distributed generation, $\bar{Z}$ is the impedance between PCC and DG system, $\bar{V}$ isthe PCC voltage. Based on this model, equation about both real and reactive power can be obtained in DG system.

The line impedance is represented as $\bar{Z} = Ze^{j\theta} = R + jX$ and the complex power which flows the transmission line is as following.

$$\bar{S} = P + Q = \bar{V}\bar{I}^{*} = V\left(\frac{E\angle\phi - V}{\bar{Z}}\right)^{*}$$

$$= \frac{VE}{Z}e^{j(\theta-\phi)} - \frac{V^2}{Z}e^{-j\theta} \tag{1}$$

$$= \frac{VE}{Z}\left(\cos(\theta-\phi) + j\sin(\theta-\phi)\right) - \frac{V^2}{Z}\left(\cos\theta - j\sin\theta\right)$$

It is considered as $\theta = 90°$because line impedances are assumed as inductive component in conventional droop method. Above equation can be simplified as following.

$$P \cong \frac{VE}{X}\sin\phi \tag{2}$$

$$Q \cong \frac{V}{X}\left(E\cos\phi - V\right) \tag{3}$$

The phase of PCC voltage ϕ can be assumed as 0 because it is very small in practice. Hence, above equations (2) and (3) can be simplified as follows:

$$\phi \approx \frac{XP}{EV}, \quad E - V \approx \frac{XQ}{V} \tag{4}$$

Equation (4) shows that the inverter phase and voltage are proportional to the real power and the reactive power, respectively (Note that the controlling the ω instead of controlling the phase ϕ has to be selected in droop control for the smoother transient dynamics and the system stability). Finally, $P-\omega$ and $Q-E$ droop control equation can be obtained as followings [5].

$$\omega^{*} = \omega_{nom} - k_{\omega}(P_{ref} - P) \tag{5}$$

$$E^{*} = E_{nom} - k_{v}(Q_{ref} - Q) \tag{6}$$

ω_{nom} : Nominal frequency, E_{nom} : Nominal voltage

ω^{*} : Reference frequency, E^{*} : Reference voltage

k_{ω} : Frequency-P droop coefficient

k_{v} : Voltage-Q droop coefficient

B. System Modeling and Virtual Inductor Method

The conventional droop has been considered as that the inductive component is dominant more than the resistive component in line impedance. But the line impedance in real system sometimes contains the resistive component somewhat in accordance with the type of system. Hence, the mutual interference component occurs in the relation between real and reactive power. Injection of the virtual inductance method to inductive-resistive complex line reduces the mutual interference so that the conventional droop method can be more effective.

Figure 2 represents the overall control scheme of droop control. As shown in this figure, the inductor current and the filter capacitor voltage have been used as a feedback. Additionally, output currents which flow the line impedance also have been used for calculations of output power and voltage drop at virtual impedance.The voltage and current controller is designed as PI-P controller and its gain has been selected through the root-locus with deliberation. But the virtual inductor voltage drop calculation with differentiation cannot be a good application because of the noise amplification due to the differentiation. Furthermore, when the inverter supplies power to the non-linear load, it becomes more serious. Hence, avoiding high frequency problem by adding the high pass filter has been researched [10, 12]. But it is not easy to select the filter cutoff frequencies and even complicated because these frequencies have to be different according to the configuration of system and load. Hence, this research adopt the simple voltage drop calculation method of virtual impedance without the differentiation by considering the complexity above mentioned [7].

$$(V_d + jV_q) = j\omega X_{\circ}\left(I_d + jI_q\right) = \omega X_{\circ}\left(-I_q + jI_d\right) \tag{7}$$

$X_{\circ}$: Virtual reactance, ω : System frequency

As shown in figure 3, the differentiation can be avoided by simplifying$sX_o$to $j\omega X_o$for the calculation of d- and q-components of reactance voltage drop. Therefore, equation (7) which adopts d-q synchronous reference frame improves the noise attenuation at high frequency.

C. Proposed Active and Reactive Power Sharing

Aforementioned in introduction, the reactive power sharing error occurs due to the unequal voltage drops when line impedances in inverter parallel operation are unbalanced. If voltage droop coefficient is very high for compensating the reactive power error, then there may be an unstable transient response and the steady-state

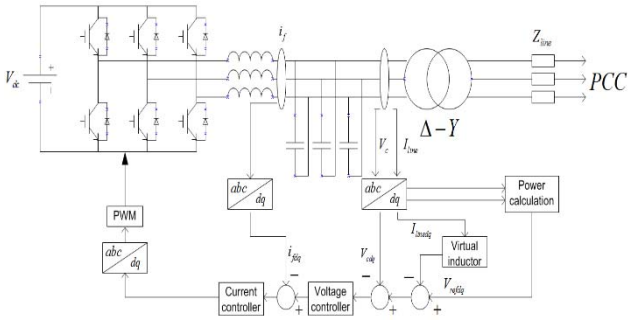

Fig. 2.Current-voltage control scheme for distributed generation interfacedwith inverter.

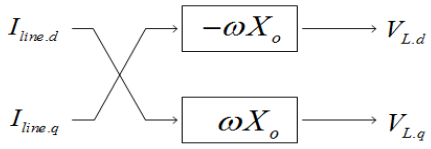

Fig. 3.Virtual inductor scheme without differentiation.

oscillations (Note that although the ramp function can be used for improving the transient dynamic, the steady state oscillation still would be exist).

In [7], the conventional droop method has been modified by using the saved information which is consist of both resistive and inductance components analyzed by the changes of real and reactive power in grid-connected mode.But this kind of analysis is quite complicated because it is difficult to know the effect of real and reactive power to the voltage drop at line impedances. Additionally, it may be necessary to use a low-pass filter for smoothening the measured real and reactive power. So in this paper, the impedance voltage drop is calculated by considering only the islanded mode firstly. And then, reference voltages are modified with these calculated variables [13]. The modified reference voltage is given as equation (8).

$$E^*_{nom} = E_{nom} + \frac{2}{3}\frac{R}{V_{PCC,peak}}P_{ref} + \frac{2}{3}\frac{Q_{ref}}{V_{PCC,peak}}(X + X_\circ) \quad (8)$$

E^*_{nom} : Proposed rated voltage

$V_{PCC,peak}$: Peak value of PCC rated voltage

By using equation (8), it can be possible to realize not only the zero steady-state error of reactive power but also the transient load sharing performance of real power. From equation (8), the voltage-reactive power droop equation can be obtained as equation (9).

$$E^*_{ref} = E_{nom} + \frac{2}{3}\frac{R}{V_{PCC,peak}}P_{ref} + \frac{2}{3}\frac{Q_{ref}}{V_{PCC,peak}}(X + X_\circ) - k_v\left(Q_{ref} - Q\right) \quad (9)$$

The detail of equation (9) is shown in figure 4. In high capacity system, the output current which flows the line is very large. Hence, it makes the voltage drop at virtual

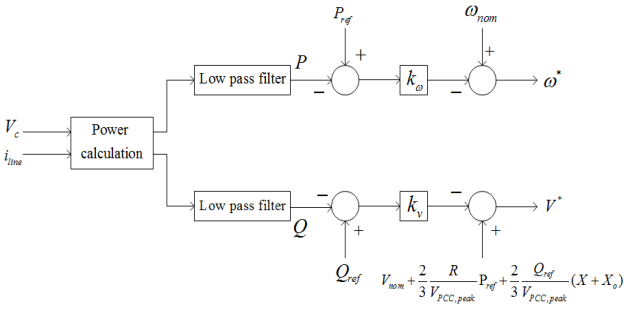

Fig. 4.Proposed droop algorithm.

inductance relatively big comparing with the nominal voltage and this causes the unrated small output power due to the reference voltage reduction by big virtual impedance voltage drop. So by using equations (8) and (9), it can be improved to meet the zero reactive power and the high performance of real power sharing.

Additionally, it can be considered the resistive droop equation when line impedances are predominantly resistive. With conventional resistive droop, the reactive power sharing is correct but real power sharing error occurs due to the unbalanced line impedance oppositely. So resistive droop equation also is proposed as (10) as like the equation (9).

$$E^*_{ref} = E_{nom} + \frac{2}{3}\frac{R + R_o}{V_{PCC,peak}}P_{ref} + \frac{2}{3}\frac{Q_{ref}}{V_{PCC,peak}}X + k_v\left(P_{ref} - P\right) \quad (10)$$

As shown in equation (10), the voltage-real power droop has been used and voltage drops of both line impedance and virtual resistor have been considered to reduce the real power sharing error.

D. Small Signal Modeling and System Stability Analysis

System stability can be analyzed by using the linearized equation of small signal modeling in transient state [14]. The conventional droop control has treated the small signal modeling without considering the virtual inductor. In this paper, the virtual inductor has been considered in small signal modeling and its validity has been checked through the MATLAB simulation referred as [11].

The DG output voltage *E*is defined as $e_d + je_q$ and the output current $e_d + je_q$is shown as equation (11).

$$i_d + ji_q = \frac{\overline{E} - \overline{V}}{\overline{Z}} = \frac{1}{Z}\left[\left(e_d - V\right)\cos\theta + e_q \sin\theta\right] - \frac{j}{Z}\left[\left(e_d - V\right)\sin\theta - e_q \cos\theta\right] \quad (11)$$

The small signal equation about current can be obtained by linearizing equation (11)

$$\triangle i_d = \frac{1}{Z}(\triangle e_d \cos\theta + \triangle e_q \sin\theta) \quad (12)$$

$$\triangle i_q = -\frac{1}{Z}(\triangle e_d \sin\theta - \triangle e_q \cos\theta) \quad (13)$$

Equation (14) can be obtained from equation (1) by transforming to dq-synchronous reference frame.

$$p + jq = V(i_d + ji_q) = V \bullet i_d - jV \bullet i_q \quad (14)$$

By using equation (11), the linearized equation of equation (14)is given as followings:

$$\triangle p = V \triangle i_d = \frac{V}{Z}\left(\triangle e_d \cos\theta + \triangle e_q \sin\theta\right) \quad (15)$$

$$\triangle q = -V \triangle i_q = \frac{V}{Z}\left(\triangle e_d \sin\theta - \triangle e_q \cos\theta\right) \quad (16)$$

Equations(7) and (8) can be transferred to equations (17) and 18 based on d-q voltage frame.

$$E_d^* = E_{nom}^* - k_v(Q_{ref} - Q) + X_\circ \frac{\omega_c}{s+\omega_c} i_q \quad (17)$$

$$E_q^* = -X_\circ \frac{\omega_c}{s+\omega_c} i_d \quad (18)$$

ω_c : Cut-off frequency of low pass filter

It is possible to change equations (5), (17) and (18) to small signal description as shown in equations (19)-(21) (Error of output and reference voltage is assumed as 0).

$$\triangle \omega = k_\omega \frac{\omega_c}{s+\omega_c} \triangle p \quad (19)$$

$$\triangle e_d = k_v \frac{\omega_c}{s+\omega_c} \triangle q + X_\circ \frac{\omega_c}{s+\omega_c} \triangle i_q \quad (20)$$

$$\triangle e_q = -X_\circ \frac{\omega_c}{s+\omega_c} \triangle i_d \quad (21)$$

Above equations are rewritten with replacing $\Delta\omega$with$s\Delta\phi$and considering low pass filter.

$$\triangle \ddot{\phi} + \omega_c \triangle \dot{\phi} = \omega_c k_\omega \Delta p \quad (22)$$

$$\triangle \dot{e}_d + \omega_c \triangle e_d = \omega_c k_v \Delta q + X_\circ \omega_c \triangle i_q \quad (23)$$

$$\triangle \dot{e}_q + \omega_c \triangle e_q = -X_\circ \omega_c \triangle i_d \quad (24)$$

Then equation (25)shows the phase of inverter ϕ and equation (26)showsΔe_q.

$$\phi = \arctan\left(e_q / e_d\right) \quad (25)$$

$$\triangle e_q = \frac{e_d^2 + e_q^2}{e_d} \triangle \phi + \frac{e_q}{e_d} \triangle e_d \quad (26)$$

Finally, the state space equation matrix can be obtained as equation (27) from the above equations.

$$\begin{bmatrix} \triangle \dot{\phi} \\ \triangle \ddot{\phi} \\ \triangle \dot{e}_d \end{bmatrix} = \begin{bmatrix} 0 & 1 & 0 \\ a & -\omega_c & b \\ c & 0 & d \end{bmatrix} \begin{bmatrix} \triangle \phi \\ \triangle \dot{\phi} \\ \triangle e_d \end{bmatrix} \quad (27)$$

where

$$a = \frac{\omega_c k_\omega V}{Z} \sin\theta \frac{e_d^2 + e_q^2}{e_d}$$

$$b = \frac{\omega_c k_\omega V}{Z}\left(\cos\theta + \frac{e_q}{e_d}\sin\theta\right)$$

$$c = \cos\theta \frac{\omega_c\left(X_\circ - k_v V\right)}{Z} \frac{e_d^2 + e_q^2}{e_d}$$

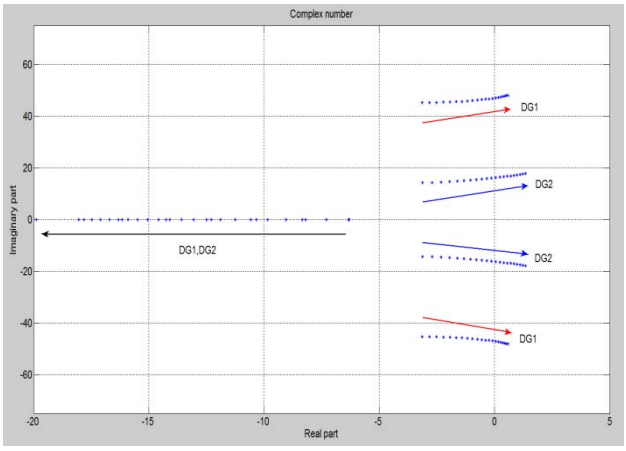

Fig. 5.System root locus with various $X_\circ$ from 0 to 1.5mH.

$$d = -\omega_c + \frac{\omega_c\left(k_v V - X_\circ\right)\sin\theta}{Z} + \frac{\omega_c\left(X_\circ - k_v V\right)\cos\theta}{Z} \frac{e_q}{e_d}$$

Equation (27) can be expressed as $\Delta\dot{X} = AX$and the system stability can be confirmed by using the value of $\Delta|sI - A| = 0$. Figure 5 represents the MATLAB simulation results based on equation (27) obtained by small signal modeling. Each parameter is same as the parameters for simulation.

It represents the root locus about the eigenvalue of state equation when the virtual inductance $X_o$changes from 0 to 1.5mH. As shown in the figure, one root moves to left side and other two roots move to stable area on the right side. The stable area of virtual inductance of DG1 is 0 to 0.265mH and it is 0 to 0.8mH for DG2. Therefore, the maximum virtual inductance can be selected as 0.265mH which satisfies the both area. Through this selected virtual inductance, the stability and the effectiveness are satisfied simultaneously. The selected virtual inductance has been adopted for PSIM simulation, too.

III. SIMULATION

Table 1 shows the parameters of parallel inverters for simulation. The virtual inductance has been selected as 0.265mH from the small signal analysis. Line impedances are intentionally unbalanced and the line impedance of DG2 is assigned as that the resistive component is more predominant than the inductive component to validate the effect of virtual inductor.

Figure 6 represents the droop performances with two parallel inverters based on the virtual inductor method for three different type of conditions (a, b, c) and the conventional droop method using high voltage droop coefficient with or without ramp function at transient state (d, e). The total simulation time is 2sec and the droop control is applied after 1sec.Figure 6(a) shows the real and reactive powers and the circulating current. Here, the unrated real power and reactive power sharing errors occur due to the big virtual impedance voltage drop and unbalanced line impedances, respectively. Figure 6(b)

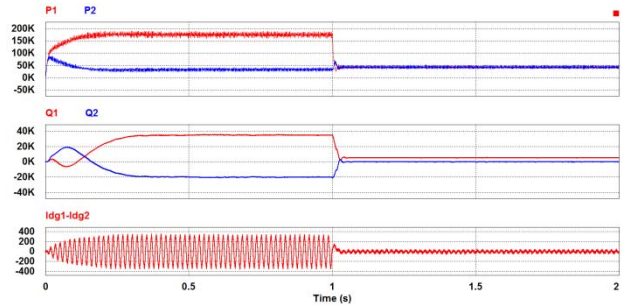

(a)

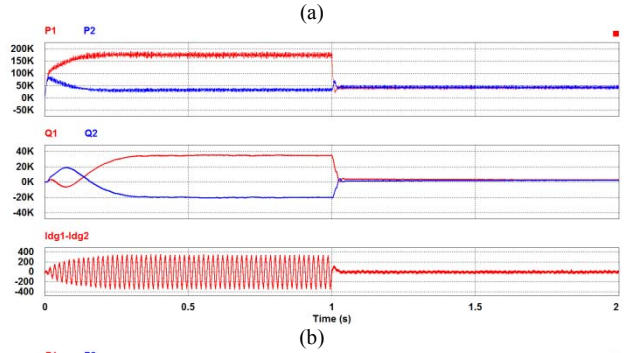

(b)

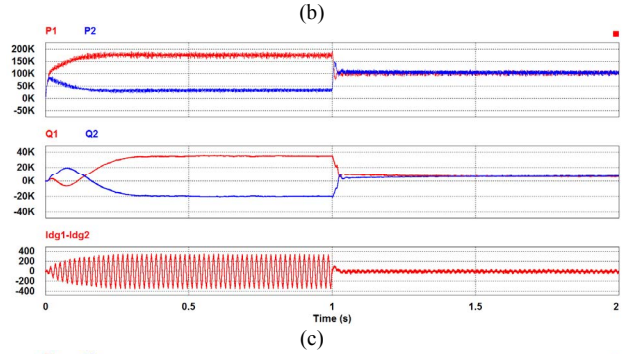

(c)

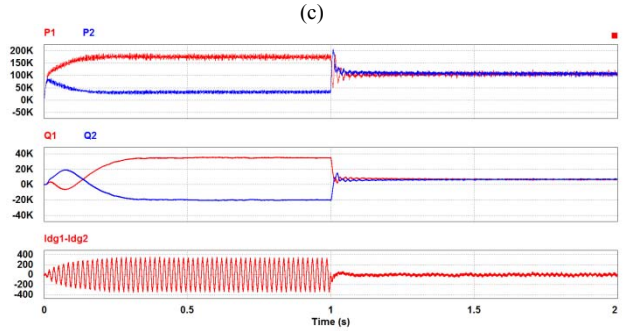

(d)

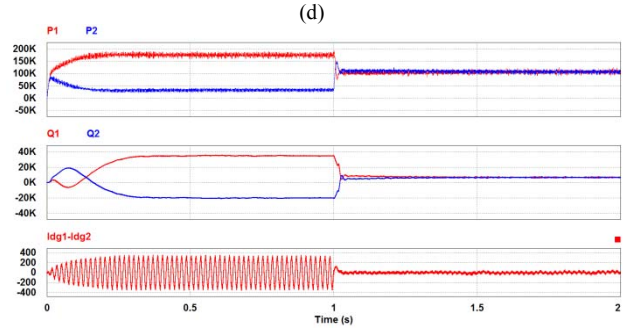

(e)

Fig. 6. Droop performances with two parallel inverters using virtual inductor method(top: active power, middle: reactive power, bottom: circulating current):(a) Conventional droop control considering equations (5) and(6), (b) droop control considering line impedance in [7], (c) proposed droop control considering virtual inductance, (d)conventional droop control using high voltage droop gain, (e) conventional droop control using high voltage droop gain with ramp function in transient.

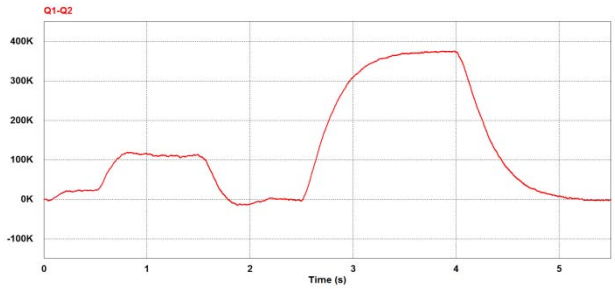

(a)

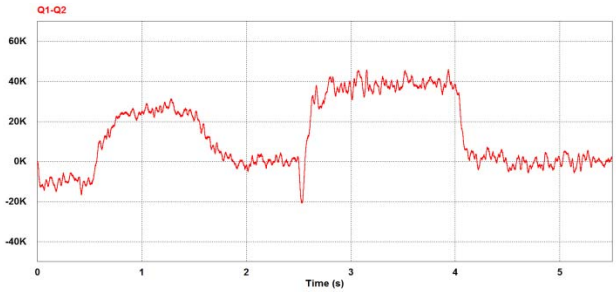

(b)

Fig. 7. Reactive power sharing errors under unequal line impedances with conventional droop control from 0.5 to 1.5sec and from 2.5 to 4sec and proposed droop control from 1.5 to 2.5sec and from 4 to 5.5sec: (a)Unequal line resistance and two times increase at 2.5sec, (b)Unequal line inductance and two times increase at 2.5sec.

TABLE I
SIMULATION PARAMETERS OF DISTRIBUTED GENERATION SYSTEM FOR DROOP CONTROLLED PARALLEL INVERTERS

Parameters	Value
P_{ref}	100 [kW]
Q_{ref}	6.6[kVar]
V_{dc}	158[V]
Frequency droopk_ω	-1×10^{-5}[rad/W]
Voltage droopk_v	-5×10^{-7}[V/Var]
Filter capacitorC_f	2100 [uF]
Filter inductanceL_f	15[uH]
DG1 line impedance	0.02[Ω], 0.08[mH]
DG2 line impedance	0.15 [Ω], 0.17 [mH]
Switching frequencyf_ω	8[kHz]
Virtual inductanceX_o	0.265[mH]

shows that the reactive power sharing error can be reduced after considering each voltage drop of unbalanced line impedances [1]. The circulating current is also reduced than that of figure 6(a). But the total value of real power sharing is still smaller than the rated real power value. Figure 6(c) adopts not only the voltage drop of line impedances but also the voltage drop of virtual inductance based on equation (9). Comparing with figure 6(b), figure 6(c) achieves the reduction of reactive power sharing error and the correct rated real power sharing simultaneously. And also, it is possible to use the high voltage droop coefficient instead of line impedance voltage drop offset as shown in figure 6(d). But its dynamic response shows some oscillations which can be assumed as unstable characteristic. So the ramp output of voltage droop has been adopted in figure 6(e) to reduce the transient droop oscillation. But although the dynamic

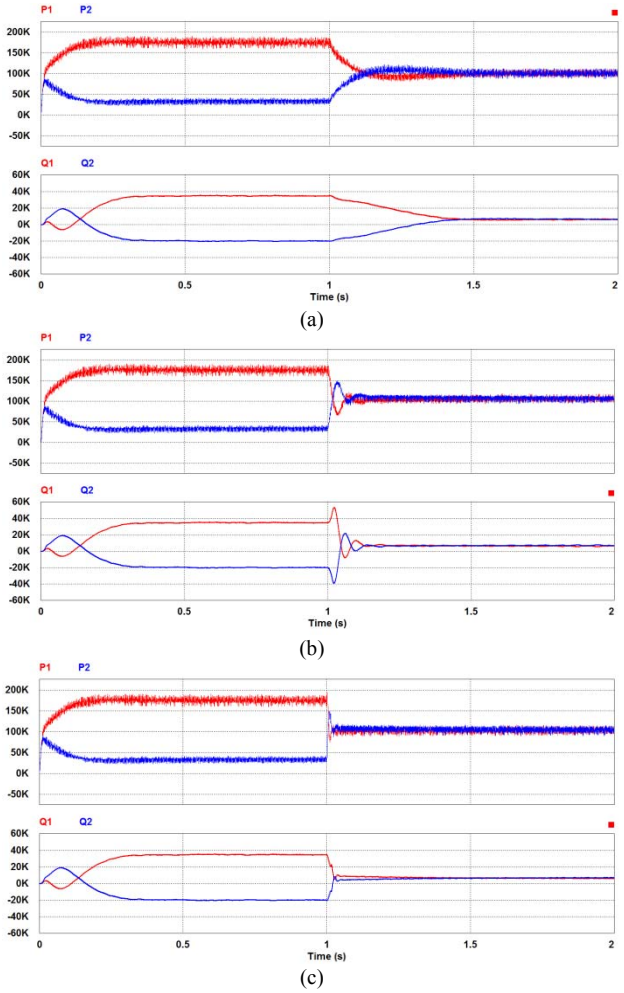

Fig. 8. Proposed droop performances with various virtual inductance (top: active power, bottom: reactive power): (a) Without*Xo*, (b)*Xo*=0.07mH, (c) *Xo*=0.265mH.

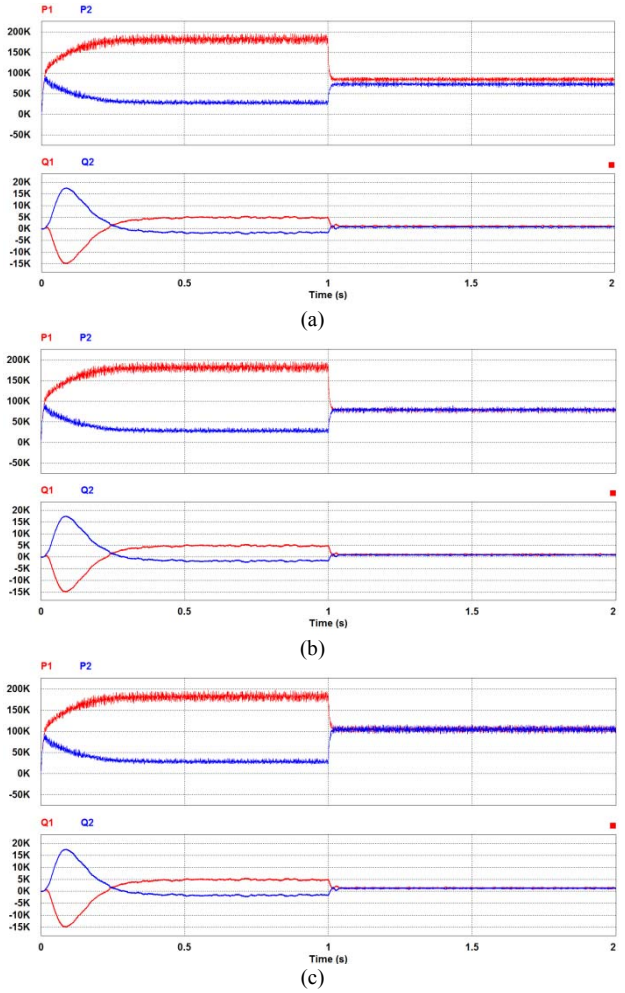

Fig. 9.Droop performance of real and reactive power with resistive droop equation (10) on resistive line(DG1: 0.03Ω and 0.008mH, DG2: 0.15Ω and 0.033mH): (a) Conventional resistive droop control, (b) resistive droop control considering only the line impedance in [1], (c) proposed droop control considering full resistive equation (10).

response can be improved to be stable with ramp function, but its steady state oscillation still occurred due to the high voltage droop coefficient. Therefore, the proposed droop method considering line impedance and virtual impedance voltage drop offset guarantees the correct real and reactive sharing performance and the system stability in both transient and steady state.

Figure 7 represents the reactive power sharing error under the different line impedance conditions. The conventional droop control is used during the periods of 0.5~1.5sec and 2.5~4sec. And the proposed droop control is used during those of 1.5~2.5sec and 4~5.5sec. In figure 7(a), the line impedance of DG1 is 0.05Ω and 0.08mH, and that of DG2 is 0.08Ω and 0.08mH, respectively till 2.5sec. After then, the line resistance of DG2 becomes two times bigger as 0.16Ω to test the validity of proposed droop performance in various line resistance condition. In figure 7(b), the line impedance of DG1 is 0.05 Ω and 0.04mH, and that of DG2 is 0.05 Ω and 0.06mH, respectivelytill 2.5sec. After 2.5sec the line inductance of DG2 becomes two times bigger as 0.12mH to test the validity of proposed droop performance in various inductive line condition. As shown in figure 7, there are reactive power sharing errors due to the unequal line impedances under the conventional droop method. But the reactive power sharing error can be reduced by using the proposed droop method regardless of various line impedances.

Figure 8 represents the real and reactive powers when the proposed droop control is adopted with three different values of virtual inductance. As like figure 6, the droop control and virtual inductor method are applied at 1sec. The virtual inductance values are 0mH, 0.07mH, 0.265mH in figures 8(a), 8(b), and 8(c), respectively. As shown in this figure, the bigger virtual inductance value, the faster and more correct sharing of real and reactive powers (Note that the excessive increase of virtual impedance which exceed right half plane on root locus causes the system instability).

Figure 9 represents the droop performances of real and reactive powers with resistive droop equation (10) on predominant resistive line. Unlike figure 6(a), the reactive power sharing is correct and the real power sharing error occurs in figure 9(a) due to the changed relation between line component and power flow. And unrated real power problem also remains same as in figure 6(a). So the line

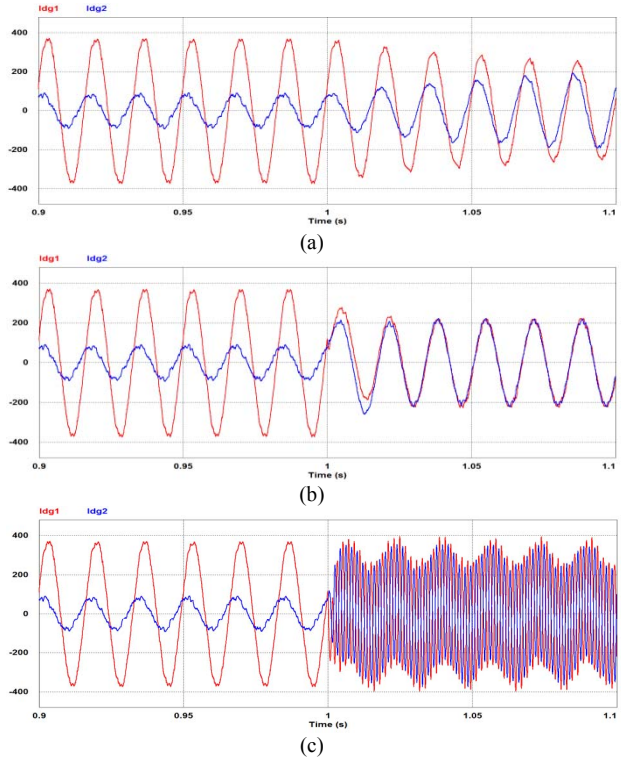

Fig. 10. Proposed droop performances with various virtual inductance (output current) (a) without Xo, (b) Xo=0.265mH, (c) Xo=0.8mH.

impedance voltage drop offset has been adopted in figure 9(b). But the shared real powers are still different from the rated value due to the high virtual impedance voltage drop. In figure 9(c), the resistive droop equation (10) has been fully adopted. As shown in this figure, the real and reactive power sharing error is almost zero and the real power rating also is recovered to its rated value.

Figure 10 represents the current waveforms under the proposed droop method with various virtual inductances. The virtual inductance value of each figure is 0, 0.265, 0.8mH, respectively. In case of figure 10(b), its sharing dynamic response is faster and more correct than that of figure 10(a). The virtual inductance of figure 10(c) is in the stable region of small signal modeling of DG2, but it is in the unstable region of small signal modeling of DG1. That is why its current waveform is unstably oscillating. Hence, the validity of small signal modeling in this paper is proved.

IV. Conclusions

The proposed droop method in this paper is based on virtual inductance selected by small signal stability analysis. Additionally, it has considered not only the voltage drops at unequal line impedances which cause the reactive power sharing error but also those at the virtual impedances which cause the rated real power reduction. Consequently, the real and reactive power sharing can be realized properly. Hence, the circulating current of inverter also has been minimized. Validities of proposed droop method and virtual impedance selection have been proved by PSIM and MATLAB simulations.

Acknowledgment

This work was supported by Chung-Cheong Institute for Regional Program Evaluation under the grant No. A004600415 <High quality high power photovoltaic based power converter system>.

References

[1] K. Lim and J. Choi, “Droop Control for ParallelInverters in islanded microgridconsidering unbalancedlow-voltage line impedance,” *Trans. of Korean Institute of Power Electronics*, vol. 18, no. 4, pp.387-396, 2013.

[2] X. Wang, J. M. Guerrero, F. Blaabjerg,and Z. Chen, “A review of power electronics based microgrids,” *Journal of Power Electronics*, vol. 12, no. 1, pp. 181-191, 2012.

[3] A. Tuladhar, H. Jin, T. Unger, and K. Mauch, “Parallel operation of single phase inverter modules with nocontrolinterconnections,” *in Conf. Rec. of IEEE APEC97*, pp. 94-100, 1997.

[4] K. S. Parlak, M. Ozdemir, and M. T. Aydemir "Activeand reactive power sharing and frequency restorationin a distributed power system consisting of two UPSunits," *Electrical Power and Energy Systems* , vol. 31,pp. 220-226, 2009.

[5] K. D. Brabandere, B. Bolsens, J. V. Keybus, A. Woyte, J. Driesen, and R. A. Belmans, “A voltage and frequency droop control method for parallel inverters,” *IEEE Trans. on Power Electron*., vol. 22, no. 4, pp. 1107-1115, 2007.

[6] J. Kim, H. Choi, and B. Cho, “A novel droopmethod for converter parallel operation,”*IEEE Trans.on Power Electron*., vol. 22, no. 1, pp. 25-32, 2002.

[7] Y. W. Li and C. N. Kao, “An accurate power control strategy for power-electronics-interfaced distributed generation units operation in a low voltage multibusmicrogrid,” *IEEE Trans. on Power Electron*., vol. 24, no. 12, pp. 2977-2988,2009.

[8] W. Yao, M. Chen, J. Matas, J. M. Guerrero, and Z. M.Qian, “Design and analysis of the droop control methodfor parallel inverters considering the impact of thecomplex impedance on the power sharing,”*IEEETrans. on Ind. Electron*., vol. 58, no. 2, pp. , 2011.

[9] K. Jung, K. Lim, D. Kim and J. Choi, “Droop method for high-capacity parallel inverters in islanded mode using virtual inductor,” *Trans. of KoreanInstitute of Power Electron*, vol. 20, vo. 1, pp. 81-90, 2013.

[10] J. M. Guerrero, L. G. Vicuna, J. Matas, M. Castilla, and J. Miret, “Output impedance design of parallel- connected UPS inverters with wireless load-sharing control,” *IEEE Trans. on Ind. Electron*., vol. 52, no. 4, pp. 1126-1135, 2005.

[11] Z. Guo, D. Sha, and X. Liao, “Wireless paralleled control strategy of three-phase inverter modules for islanding distributed generation systems,” Journal of Power Electronics, vol. 13, no. 3, pp. 479-486, 2013.

[12] J. M. Guerrero, L. G. Vicuna, J. Matas, M. Castilla, and J. Miret, “A wireless controller to enhance dynamic performance of parallel inverters in distributed generation systems,” *IEEE Trans. on Power Electron*., vol. 19, no. 5, pp. 1205-1213,2004.

[13] J. He and Y. W. Li, “Analysis, design, and implementation of virtual impedance for power electronics interfaced distributed generation,” *IEEE Trans. Ind. Appl*., vol. 47, no. 6, pp. 2525-2538,2011.

[14] C. K. Sao and P. W. Lehn, “Autonomous load sharing of voltage source converters,” *IEEE Trans. on Power Delivery*, vol. 20, no. 2, pp. 1009-1016, 2005.